Journal of Polymer Research (2022) 29: 314
https://doi.org/10.1007/s10965-022-03170-8

ORIGINAL PAPER

A facile synthesis and dual stimuli-responsive properties of BSA-based core–shell microspheres

Xiangyuan Wang[1] · Chongwu Mao[1,2] · Quanfang Li[3] · Rongmin Wang[1]

Received: 14 December 2021 / Accepted: 30 June 2022 / Published online: 8 July 2022

Abstract

A kind of novel thermal and pH stimuli-responsive core-shell microspheres (BSA@PVP) based on bovine serum albumin (BSA) have been synthesized via *in-situ* polymerization of N-vinyl pyrrolidone (NVP), and subsequent self-assembly in aqueous solution. The structure and morphology of the BSA@PVP microspheres were characterized by FT-IR, TEM and DLS. The changes of size and carried charges in response to temperature and pH value were assessed using UV-Vis spectra and DLS. The drug release behaviors were investigated under different conditions. The results indicated that the composites have core-shell structure, the diameter is about 0.15-0.35 μm and the negative charges are carried. These microspheres exhibited a continuous controllable release of the entrapped doxorubicin hydrochloride (Dox·HCl) for about 50 h. They were a kind of potential dual stimuli-responsive drug carrier. BSA@PVP microspheres exhibit high release rate in acidic environment that may be helpful to achieving a required placid level and rapidly controlling illness. Accordingly, there is a lower release rate in alkaline environment, which may be conducive to avoid the sudden release and maintain plasma concentration for a long time.

Keywords Dual stimuli-responsive · Core-shell microsphere · Drug carrier · Poly(vinyl pyrrolidone) · BSA

Introduction

Bio-polymeric microsphere is a kind of excellent new functional materials in the medical field due to its favorable biocompatibility and biodegradability. It can encapsulate large quantities of guest matters and release them in a controlled manner. As being added the incorporate functional units, it can self-test, self-judgment and self-dealing on the whole [1–3]. As a smart material [4], it not only plays an important role in drug controlled release system [5], but also has a considerable prospect in harmful metal ions detection [6] and separation [7–9], immunoassay [10], cell separation [11], advanced cosmetics [12], environment-friendly high-performance catalysts [13, 14] and other related fields [15–19]. Some methods, such as the self-assembly of block copolymers in selective solvent [20, 21], layer-by-layer deposition of polyelectrolytes on sacrificial core [22, 23], and microemulsion as well as miniemulsion polymerization [24, 25], have been developed to fabricate core-shell polymeric spheres [26].

Bovine serum albumin (BSA) is a versatile protein. It is non-antigenic, biodegradable, and readily available. Albumin has been used as materials for preparation of microspheres because it has a remarkable ability to bind a wide range of insoluble endogenous and exogenous compounds [27–29]. Currently, there have been great interests in exploiting the shuttle protein carrier for the development of novel therapeutic reagents used as drug delivery [30, 31] and novel hydrophilic carriers [32, 33]. Poly(vinyl pyrrolidone) (PVP) is a biodegradable and water-soluble synthetic polymer. It can be used to prepare polymeric microspheres in aqueous solution [34, 35]. Now, it has attracted more and more attention in the fields of medicine and pharmaceutics due to its ability to bind reversibly various molecules (dyes, metals

✉ Rongmin Wang
wangrm@nwnu.edu.cn

[1] Key Lab. Eco-Functional Materials of MOE, Institute of Polymer, College of Chemistry and Chemical Engineering, Northwest Normal University, Lanzhou 730070, China

[2] College of Chemical Engineering, Sichuan University of Science & Engineering, Zigong 643000, China

[3] Key Lab. Evidence Science of Gansu Province, Gansu University of Political Science and Law, Lanzhou 730070, China

and some polymers) in solution [36] and excellent biocompatibility with living tissue [37] and low cytotoxicity [38].

Temperature and pH value are important factors in physical, biological and chemical systems, they are vital stimulus signals to obtain and operate easily, either. In complex body systems, drugs are stimulated by both temperature and pH value. Obviously, single factor responsive materials cannot meet the functional requirements in biological and pharmaceutical fields. Therefore, it is necessary to develop a new kind of material which has multiple responses performance under different external stimuluses at the same time. As a result, temperature and pH value sensitive materials have increasingly attracted the attention of researchers.

In this paper, a novel BSA-based microsphere (BSA@PVP) was prepared via *in-situ* polymerization of N-vinyl pyrrolidone (NVP) and subsequent self-assembly. We employ BSA as the biomaterial which has a lot of hydrophilic groups, such as 116 amino, 99 carboxyl, and vinyl pyrrolidone (NVP) as functional monomer. Due to PVP chains could dissolve in pure water, the phase transition wouldn't happen if the temperature is lower than the boiling point of water [39]. Therefore, hydrogen bonds or polar bonds would be achieved around the albumins' skeleton by absorbing a lot of PVP chains. That can further improve the temperature and pH sensitive properties of drug carrier. Their structure, morphology and particle size was characterized by the Fourier transform infrared (FT-IR), transmission electron microscopy (TEM), dynamic light scattering (DLS), and ultraviolet–visible (UV-Vis) spectra. Its dual stimuli-responsive properties to temperature and pH value and controllable drug release behavior have also been investigated.

Experimental

Materials and measurements

BSA was purchased from Shanghai Boao Bio. tech. Co. Ltd. Vinyl pyrrolidone (NVP) was obtained from Tianjin Guangfu Chem. Res. Inst., and was purified before use. Azobisisobutyronitrile (AIBN) was recrystallized before use. Doxorubicin hydrochloride (Dox·HCl) was purchased from McLea Bio. Tech. Co. (Shanghai, China). All other reagents are analytical grade and were used without further purification unless otherwise specified. Double-distilled water was used throughout this work.

The chemical interaction between BSA and PVP was studied by FT-IR Spectrometer (Alpha-Centauri, Mattson, USA). These obtained microspheres were mixed with potassium bromide (KBr) at a ratio of 1:100 by grinding and pressed into pellets for measurement.

TEM images of the as-synthesized microspheres were obtained on a transmission electron microscope (JEM-1230, JEOL). The sample was stained with 2.5% phosphotungstic acid (PTA) solution, then added on a copper grid in drops, which was placed in a Petri dish covered with a filter paper, and dried at room temperature for 3 min.

Hydrodynamic diameter, size distribution and ξ-potential of the BSA@PVP microspheres were detected using a DLS particle size analyzer (Zetasizer Nano ZS, Malvern, UK).

The content of drug in solution was detected by a UV–Vis spectrophotometer (Agilent 8453, Agilent, USA).

Synthesis of BSA@PVP microspheres

Firstly, a certain amount of AIBN was added into 4 mL of NVP solution. After being stirred for 15 min, 100 mL of BSA solution (10 mg·mL^{-1}) was added, and then the mixture was stirred for 30 min at 55 °C under nitrogen atmosphere. The *in-situ* polymerization of NVP around the skeleton of BSA and the subsequent self-assembly had proceeded for 3 h at the same temperature. After being cooled to room temperature, the resulted solution was dialyzed three times (MW cutoff 10 kDa) against the aqueous solution (W_t = 1:100) to remove the small molecular substance and dissociative PVP oligomers. After being lyophilized, the light yellow powder solid samples of BSA@PVP microspheres were obtained.

Dual stimuli-responsive properties of BSA@PVP

The normal temperature of the human body is about 37 °C. Drugs containing protein components are usually stored at about 0 °C. The pH value of human blood is about 7.4. The pH value in the stomach after meals is about 3.0. Therefore, we set the test temperature at 0 °C, 15 °C, 25 °C and 37 °C and pH value at 7.4 and 3.6 to investigate the thermal and pH dual stimuli-responsive properties of BSA@PVP. The particle size analyzer was employed to assess sizes, and changes of carried charges in response to temperature and pH value. In the process of detection, DTS1060 type sample cell was employed, the scattering angle was 900, and the test temperature was 25 °C. The pH of BSA@PVP solutions were adjusted using HCl solution (1.0 mol·L^{-1}) or NaOH solution (1.0 mol·L^{-1}). At each test point, experiments were conducted in triplicate.

The release behaviors of drug loaded BSA@PVP microspheres

The aliquots of drug-loaded microspheres were prepared as follows: Firstly, 5 mg of drug was dissolved in 5 mL of BSA@PVP solution as one sample; Then, the solution was oscillated for about 10 h at room temperature to disperse the drug into microspheres adequately. The effects of temperature and pH value on their drug release behavior were investigated. The drug encapsulation efficiency (DrugEE:

(%, w/w)) and drug loading capacity (DrugLC: (%, w/w)) of BSA@PVP microspheres in saline solution at 37 °C were calculated based on following formulas:

$$DrugEE(\%, w/w) = [(WTdrug - Csol \times Vsol)/WTdrug] \times 100\% \quad (1)$$

$$DrugLC(\%, w/w) = [(WTdrug - Csol \times Vsol)/Wcrs] \times 100\% \quad (2)$$

$$mdrug(mg) = WTdrug \times DrugEE \quad (3)$$

where WTdrug (mg) is the total amount of drug in each sample; Wcrs (mg) is the amount of dried carrier; Csol (mg·mL-1) is the concentration of the solution after drug load; Vsol (mL) is the volume of the solution after drug load; mdrug (mg) is the amount of drug loaded into the carrier.

Because the sizes of microspheres are very small, the dynamic dialysis method was employed to carry out drug release test, and the phosphate buffer solution (PBS, 0.02 M) was employed as dialysis medium (MW cutoff 3500). The amount of released drug was detected by UV-Vis spectrometer. The release rates under different temperatures and different pH conditions are calculated based on the initial amount of drugs in the microspheres:

$$Released\% = [CRsol \times VRsol/mdrug] \times 100\% \quad (4)$$

where CRsol (mg·mL^{-1}) is the drug concentration in the release medium after the drug was released for a certain period of time; VRsol (mL) is the volume of the release medium; mdrug (mg) is the amount of drug loaded into the carrier.

Results and discussion

Formation process of BSA@PVP core-shell microspheres

The BSA@PVP microspheres were prepared by *in-situ* polymerization and subsequent self-assembly of NVP in BSA aqueous solution (Scheme 1). A logical formation process of the BSA@PVP core-shell microspheres is designed, outlined in Scheme 1. Firstly, BSA and NVP are both readily soluble in water. NVP was dispersed in BSA solution

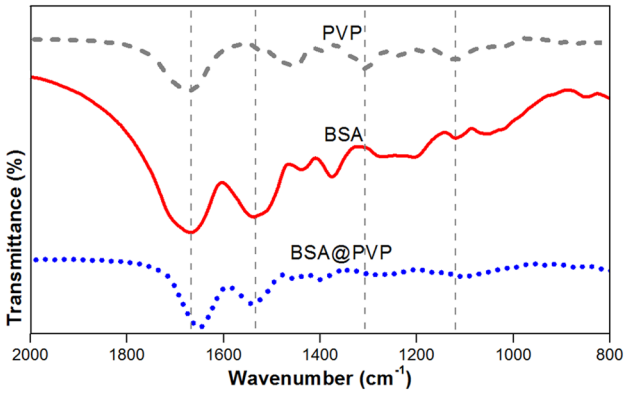

Fig. 1 FT-IR spectra of BSA, PVP and BSA@PVP

with hydrogen bonds or polar bonds. A p-π conjugation system is formed between the lone pair electrons of the amide bond (-CO-NH-) nitrogen atom and the C-O bond. Due to the delocalization of electron pairs on N atoms, the bond length of C-N bond is shorter than that of amines, and it has the property of partial double bond. In addition, oxygen's electron-sucking effect also reduces the density of electron clouds on nitrogen, thus reducing the alkalinity of nitrogen. Then, NVP in-situ polymerized around the skeleton of BSA (Scheme 1). At the moment, the short PVP chains should be completely water-soluble. Secondly, with the propagation of PVP chains, the high-molecule began to self-assemble under the electrostatic attraction and hydrogen bonding between the amino and carboxyl as well as the keto. Phase transition phenomenon was observed when the PVP chains reached a certain critical length (Figs. 1 and 2). Figure 1 indicated that the microspheres is core-shell, and the center is darker than the margin. This phenomenon demonstrates that the core is denser than the shell. As the aggregation of PVP chains had happened, the PVP chains were separated from the water phase, and then the elementary particles formed. Then, with PVP chains entering through BSA skeleton, a semi-interpenetrating polymer network thus formed. Simultaneously, along with the branching and cross-linking of PVP chains around those particles, a water-insoluble core formed (Fig. 1). Thirdly, the PVP chains gathered on the surface of core, and thus the shell was produced through

Scheme 1 Schematic illustration of formation process of BSA@PVP core-shell microspheres

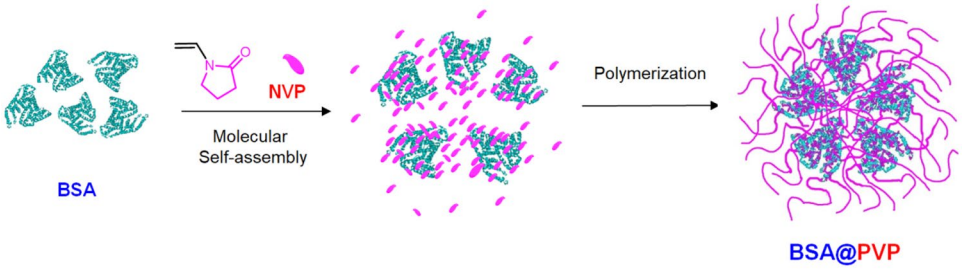

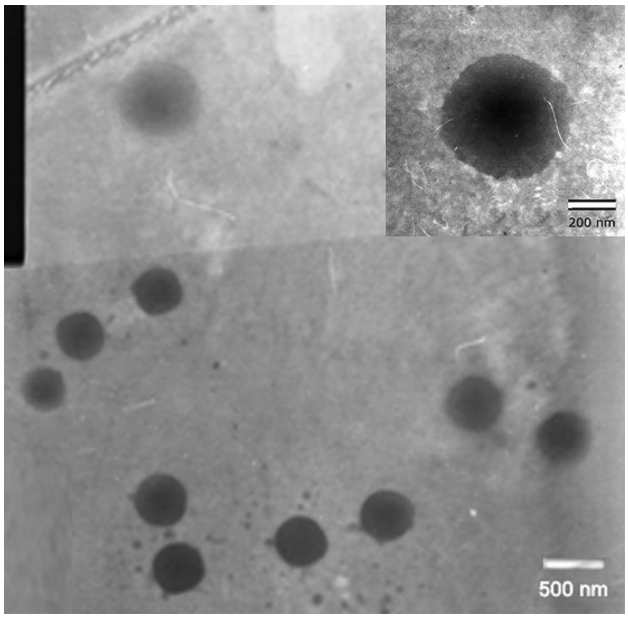

Fig. 2 TEM micrograph of undried BSA@PVP microspheres

various interactions between the hydrophilic groups, including hydrogen bonds, electrostatic force and other forms of bonds (Scheme 1, Fig. 1). Finally, some matters, such as NVP, initiators, and dissociative PVP oligomers were isolated by dialysis. BSA@PVP microspheres were soft and flexible and could be uniformly dispersed in the aqueous solution (Figs. 1 and 2).

FT-IR analysis

Figure 1 shows the FT-IR spectra of BSA@PVP. It can be observed clearly in infrared spectrum, the characteristic absorption peaks of amide band I and II shift from 1668 and 1536 cm^{-1} of pure BSA to 1656 and 1545 cm^{-1} of BSA@PVP, the intensity of absorption peak at 1656 cm^{-1} is strong. It is attributed to the superimposition of amide band I peaks of BSA and the ketos peak of PVP. The peaks shift from 1309 and 1121 cm^{-1} of pure PVP to 1274 and 1092 cm^{-1} of BSA@PVP, respectively. It is confirmed that the interaction of hydrogen bonds are produced between the amino of BSA and the carbonyl of PVP.

Morphology of BSA@PVP

TEM was employed to observe the morphologies of BSA@PVP. In order to improve visibility, PTA was adopted to stain microspheres. Figure 2 shows a typical TEM micrograph of stained BSA@PVP. It can be observed that the diameter of BSA@PVP is about 0.2-0.4 μm, the structure of BSA@PVP microspheres is core-shell, and the color of the center is darker than that of the margin. This phenomenon demonstrates that the core is denser than the shell, which is consistent with the description of reaction process and the core-shell structure of BSA@PVP.

Stimuli-responsive property of BSA@PVP

In human body, some factors, such as pH value, temperature, ionic level and blood sugar level, can influence drug efficacy. If the drugs can respond to the complex and changing internal environment within living body, it is undoubted that the best effects of drugs can be achieved to maximize the therapeutic effects while minimize the adverse reactions. The well-designed polymer BSA@PVP microspheres with special structures were expected to help drugs achieve this goal.

Temperature stimuli-responsive behavior of BSA@PVP

Temperature plays an important role in pharmacodynamics. Temperature-induced drugs can enhance the curative effect on tumor cells while reduce the toxic and side effects on normal cells. Therefore, as drug carriers, the temperature stimuli-responsive behaviors of obtained BSA@PVP microspheres were investigated. Figure 3 shows the effect of temperature on the particle size (a), ξ-potential (b) and polymer dispersity index (PDI) (c) of BSA@PVP. It can be observed that the diameter of BSA@PVP is increased from 0.18 to 0.23 μm as well when the temperature is risen from 10 °C to 25 °C. However, the size of BSA@PVP microspheres appears a sudden decrease (Fig. 3a) when the temperature reaches 30 °C. Meanwhile, the ξ-potential of BSA@PVP microspheres decreases monotonously when the temperature is risen from 10 °C to 25 °C, and there is a sudden increase when the temperature rises to 30 °C (Fig. 3b). The reasons are analyzed as follows: with the increasing of temperature, the motion velocity of water molecule in the system was accelerated and the protonation of carboxyl was enhanced. At that time, the structure of BSA@PVP was maintained through the interaction of non-covalent bonds, which include electrostatic repulsion of $-COO^-$ groups, hydrogen bonds and hydrophobic interaction of PVP chains. The hydrogen bond plays a major role in the system, and the PVP chains are soft and extend in the water. In the procedure of swelling and permeation, water molecules entered into the microspheres, as a result, the size of microspheres increased and the ξ-potential decreased. While the temperature was risen to the critical point (30 °C), the soft and extended PVP chains exhibited a typical phase separation and formed a hydrophobic region (coil-globule). Then, the hydrogen bonds were destructed and the hydrophobic interaction

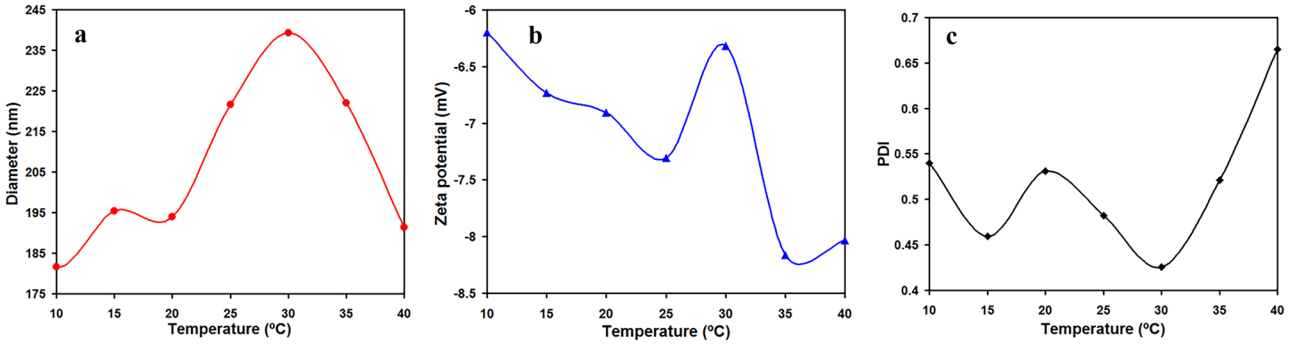

Fig. 3 Effects of the temperature to size **a**, zeta potential **b** and PDI **c** of BSA@PVP microspheres

played a major role. While the BSA@PVP microspheres contracted, water molecules would be squeezed out, which would result in decrease of the microsphere size and increase of the *ξ*-potential.

To some extent, the PDI can illustrate the uniformity of particle size. The PDI of BSA@PVP shows serrate change, when the temperature is risen from 10 °C to 30 °C. The PDI value is the minimum when the temperature is at 30 °C, which suggested that the particle sizes are almost uniform. Subsequently, along with the continuous rise of temperature, the PDI is also increased. It indicates that the particle size is non-uniform (Fig. 3c). At the same time, if the single microsphere contracts, the hydrophobic action will lead to the aggregation of BSA@PVP and form larger aggregates, so the PDI is increasing correspondingly [40]. The variation of PDI is associated with that of the size and ξ-potential of the microspheres. Therefore, It is concluded that the optimal temperature is about 30 °C.

pH stimuli-responsive behavior of BSA@PVP

It is found that the size of BSA@PVP presents a serrate change with the increasing of PH value (Fig. 4a). When the pH value is increased from 2.0 to 4.2, the diameter of BSA@PVP decreases from 0.15 μm to 0.08 μm, and then increases from 0.08 μm to 0.42 μm, as a result, there is a minimum diameter 0.08 μm. When the pH value is varied from 5.0 to 6.6, the diameter of BSA@PVP increases from 0.37 μm to 0.41 μm, and then decreases from 0.41 μm to 0.29 μm, as a result, there is a maximum diameter 0.41 μm. The ξ-potential of BSA@PVP also shows a serrate change, moreover, the ξ-potential maintains the positive value when the pH is lower than 4.2, and it is negative when the pH is higher than 5.8 (Fig. 4b). The BSA@PVP aggregates when the pH value is 4.2-5.8, and uniformly disperses again when the pH is higher than 5.8.

Figure 5 shows the photos of BSA@PVP solution in different pH conditions. When the pH value is 4.2, the white

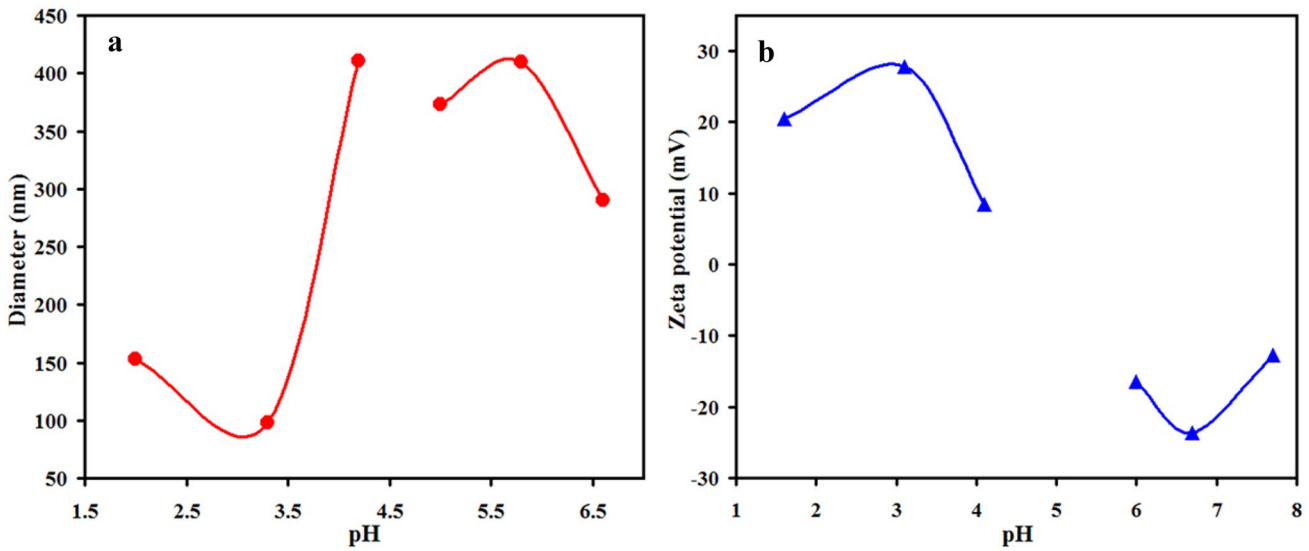

Fig. 4 Effects of the pH value to size **a** and zeta potential **b** of BSA@PVP microspheres

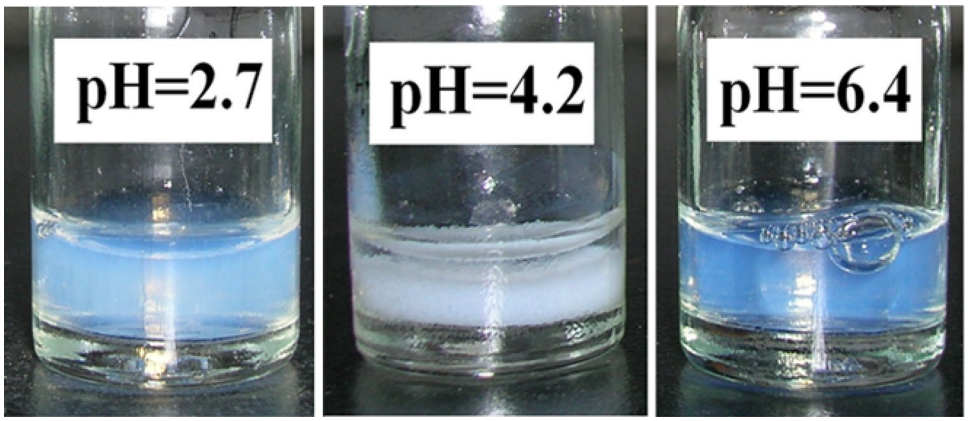

Fig. 5 Photos of BSA@PVP solution in different pH conditions

precipitate appears in solution. It is considered that the aggregation of BSA@PVP occurs when the pH value is 4.2, due to the pH in the system is close to the isoelectric point of BSA (pI = 4.7). In this case, the ξ-potential of the microspheres is almost to zero. And the electrostatic repulsion between the microspheres was lost. Thus, the microspheres appear aggregation.

In addition, due to the amino protonation in acidic environment, hydrogen bonds and electrostatic attraction are weakened. The microspheres become loose, which helps water molecules penetrate into the microspheres. As is shown in Fig. 4, the particle diameter is increased and the ξ-potential is decreased while the pH value varies from 3.6 to 2.2. Contrasted to those of pH value varying from 3.6 to 2.2, the diameter and ξ-potential exhibit the significant changes when the pH varies from 3.6 to 4.2. It can be attributed to the more isoelectric point aggregation of water molecules penetration. The variation of BSA@PVP ξ-potential (Fig. 4b) in response to pH indicates that the surface of microspheres should mainly be composed by BSA and PVP, and the long PVP chains form the core of core-shell microspheres, which is also confirmed by the reaction process and core-shell structure of BSA@PVP.

Drug-release behavior of BSA@PVP

Doxorubicin hydrochloride (Dox·HCl) is a kind of widely used drug in cancer chemotherapy. However, it is difficult to keep a stable and lasting plasma concentration due to the burst. Here, the BSA@PVP was employed as microcapsule to encapsulate Dox·HCl to keep plasma concentration. Figure 6 shows the release profiles of Dox·HCl from BSA@PVP in saline solution at 37 °C, with an average DrugEE (%, w/w) being 85.3% and DrugLC (%, w/w) being 2.87%. Although it is demonstrated that the burst release behavior is for the initial 6 h, the entrapped Dox·HCl could be continuously released up to 50 h. It is also demonstrated that there is an obvious slow-release effect compared with the blank control samples (physiological saline and BSA solution).

Drug-release of BSA@PVP in response to temperature

Figure 7 shows the release profiles of Dox·HCl from BSA@PVP microspheres at different temperatures. It is found that the drug releases of BSA@PVP microspheres at 0 °C and 15 °C show the monotonous increases in response to the different temperature within 50 h. This change is consistent with the law that the movement of water molecules can be accelerated with the increase of temperature under normal circumstances, and the drug release will increase accordingly.

It is shown that the drug releases at 25 °C and 37 °C appear the obvious rise within 10 h. Then they keep the stable rules with about a release rate of 80% at later stage. It is shown that the release rate at 37 °C is especially lower than that at 15 °C when the drug release time reaches 50 h. It is considered that the PVP chains present irregular curl at about 30 °C, which results in the contraction of the whole microspheres and the decrease of their size. Even more serious, some microspheres collapsed or partly aggregated. A

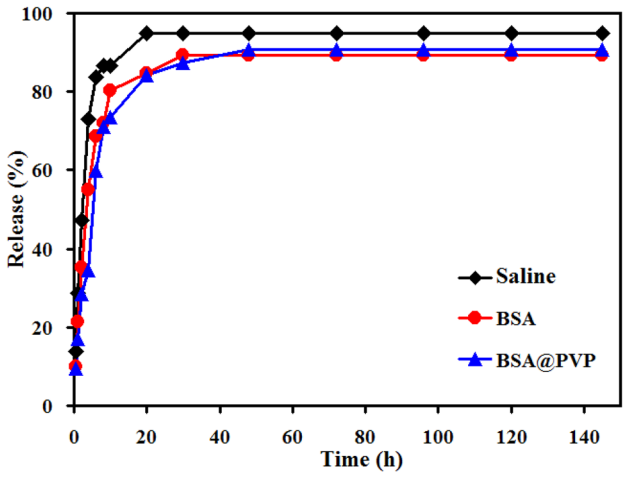

Fig. 6 Release profiles of Dox·HCl from BSA@PVP microspheres in saline solution at 37 °C

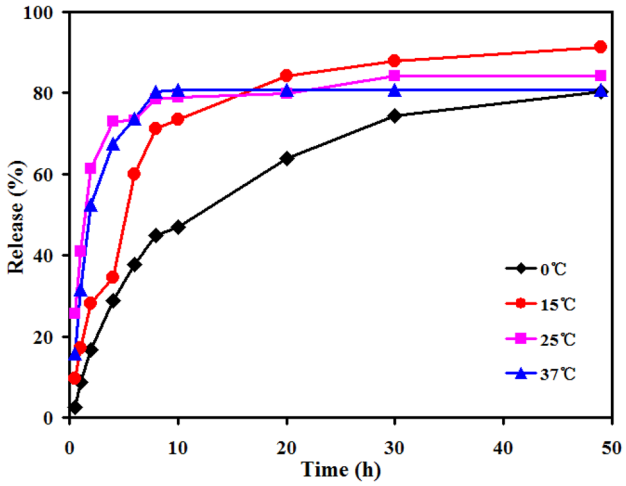

Fig. 7 Release profiles of Dox·HCl from BSA@PVP microspheres in double-distilled water at different temperature

certain amount of drugs were wrapped into those collapsed or aggregated microspheres, thus, once the drugs on the surface were completely released, it would be difficult that the drugs in the collapsed or aggregated space were released. As a result, the drug release at 37 °C was kept stable after 10 h. The phase transition did not occur at 0 °C and 15 °C, therefore, the drug release rate was kept a continuous rise.

After a careful observation, it was found that the drug release rate at 25 °C is faster and higher than that at 37 °C within 4 h. It had no phase transition at 25 °C at the beginning, which resulted in the faster drug release at 25 °C than that at 37 °C within 4 h. At 25 °C, the mild phase transition could appear while the release time was extended. Therefore, the drug release rate no longer increased monotonously just like it at 0 °C and 15 °C, but were kept a stable state like it at 37 °C. From above phenomenon, it was concluded that BSA@PVP is more likely to present a continuous phase transition rather than non-continuous phase transition.

The size of BSA@PVP microspheres appears obvious reduce at around 30 °C (Fig. 4). This indicates that the phase transition occurred at around 30 °C. Meanwhile, the drug release behaviors at different temperature also proved the existence of phase transition. So it can be confirmed that the BSA@PVP microspheres have obvious thermo-responsive property.

Drug-release of BSA@PVP in response to pH values

The release profiles of Dox·HCl from BSA@PVP in different pH values at 37 °C are shown in Fig. 8. The drug releases of BSA@PVP demonstrate a regular increase with pH value varying from 3.6 to 7.4. When the pH is 3.6, protonation of BSA was enhanced; the hydrogen bonding between the amino and the PVP chains was weakened. The BSA@PVP microspheres became loose, meanwhile, the drug release became easier. When the pH is 7.4, the microspheres are tight, drug diffusion resistance increases, drug release rate

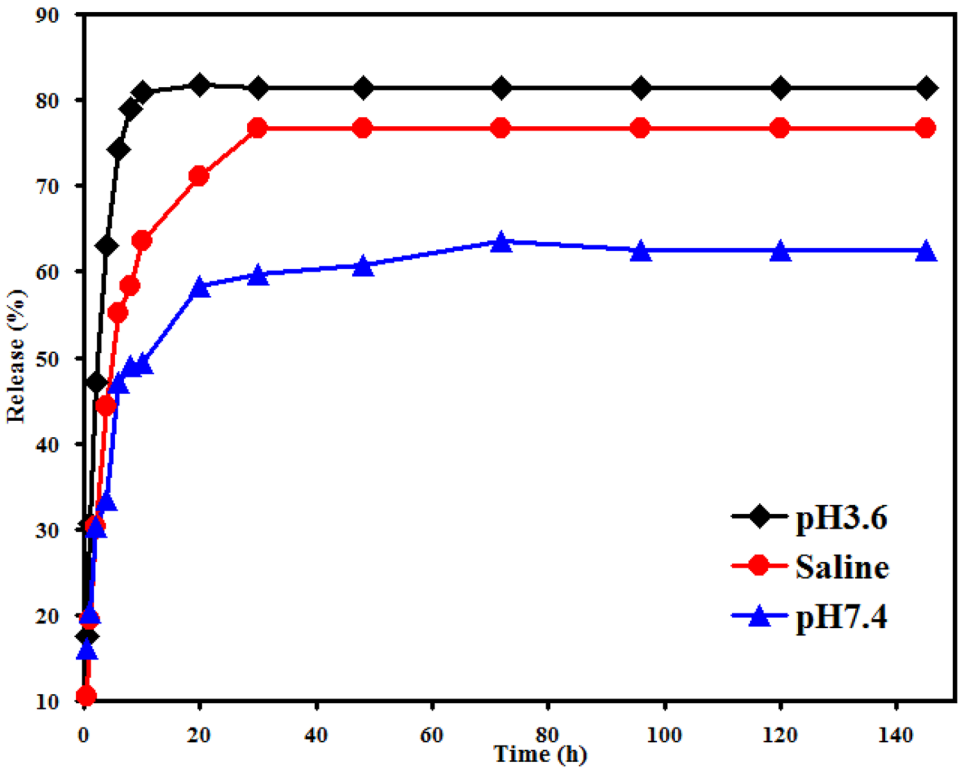

Fig. 8 Release profiles of Dox·HCl from BSA@PVP microspheres at different pH condition at 37 °C

obviously becomes lower than that of pH at 3.6. In physiological saline, BSA@PVP microspheres are stable, drug release rate is moderate. At that time, the absolute value of charge carried by the microspheres was the largest, they were more evenly dispersed in solution due to electrostatic repulsion, and the drug was constantly diffused from them. In conclusion, the drug release behaviors of BSA@PVP microspheres in different pH environment also confirm that they have pH sensitivity property.

Conclusions

In summary, the *in-situ* polymerization and self-assembly methods were adopted to synthesize a kind of novel BSA@PVP microspheres. The diameter of microspheres is about 0.2-0.4 μm. This microspheres have special core-shell structure and soft, flexible properties. They can be easily impregnated drugs or other substances. They also have the temperature and pH sensitive properties. There are close relations between the sizes, electric charges and drug release behaviors of BSA@PVP microspheres under the different temperature and pH conditions. As drug carriers, BSA@PVP microspheres exhibit high release rate in the acidic environment, which may be helpful to achieving a required placid level and rapidly controlling illness. Accordingly, there is a lower release rate in alkaline environment, which may be conducive to avoid the sudden release and maintain plasma concentration for a long time. BSA@PVP core–shell microspheres have dual stimuli-responsive properties and biocompatible skeleton, which will make it become an attractive candidate for applications in medicinal and biomedical fields.

Acknowledgements This work is supported by National Natural Science Foundation of China (21865030).

Declarations

Conflict of interest The authors declare that they have no actual or potential conflict of financial interest.

References

1. Hu X, Zhang Y, Xie Z, Jing X, Bellotti A, Gu Z (2017) Stimuli-responsive polymersomes for biomedical applications. Biomacromol 18:649–673
2. Wang J, Qian W, He Y, Xiong Y, Song P, Wang R (2017) Reutilization of discarded biomass for preparing functional polymer materials. Waste Manage 65:11–21
3. He Y, Yan G, Xu Z, Wang J, Qian W, Wang R (2017) SPI/CS nanoparticles conjugating amino acid schiff-base metal complexes for mimic of SOD. J Control Release 259:e182–e183
4. Wang X, Cheng R, Cheng L, Zhong Z (2018) Lipoyl ester terminated star PLGA as a simple and smart material for controlled drug delivery application. Biomacromol 19:1368–1373
5. Wang D, Xia Y, Zhang D, Sun X, Chen X, Oliver S, Shi S, Lei L (2020) Hydrogen-bonding reinforced injectable hydrogels: Application as a thermo-triggered drug controlled-release system. ACS Appl Polym Mater 2:1587–1596
6. Samanta SK, Dey N, Kumari N, Biswakarma D, Bhattacharya S (2019) Multimodal ion sensing by structurally simple pyridine-end oligo p-phenylenevinylenes for sustainable detection of toxic industrial waste. ACS Sustain Chem Eng 7:12304–12314
7. Liu L, Zhang K (2018) Nanopore-based strategy for sequential separation of heavy-metal ions in water. Environ Sci Technol 52:5884–5891
8. Li X, Wang B, He Y, Song P, Yan G, Wang R (2021) Soybean protein isolate-based microgels bounding amino acid metal complexes for scavenging superoxide anion radicals. Polym Bull 78:713–728
9. Wang J, Li X, He Y, Song P, Wang R (2018) Preparation of keratin-glycine metal complexes and their scavenging activity for superoxide anion radicals. Int J Polym Sci 2764749:1–8
10. Yang Z, Cao Y, Li J, Lu M, Jiang Z, Hu X (2016) Smart CuS nanoparticles as peroxidase mimetics for the design of novel label-free chemiluminescent immunoassay. ACS Appl Mater Inter 8:12031–12038
11. Zhang X, Zhu Z, Xiang N, Long F, Ni Z (2018) An automated microfluidic instrument for label-free and high-throughput cell separation. Anal Chem 90:4212–4220
12. Deb A, Saikia R, Chowdhury D (2019) Nano-bioconjugate film from aloe vera to detect hazardous chemicals used in cosmetics. ACS Omega 4:20394–20401
13. Bie S, Du M, He W, Zhang H, Yu Z, Liu J, Liu M, Yan W, Zhou L, Zou Z (2019) Carbon nanotube@RuO_2 as a high performance catalyst for Li-CO_2 batteries. ACS Appl Mater Inter 11:5146–5151
14. Wang R, Wang H, Wang Y, Li H, He Y, Hao E (2014) Preparation and photocatalytic activity of chitosan-supported cobalt phthalocyanine membrane. Color Technol 130:32–36
15. Lewis DH (1990) in: Chasin M, Langer R (eds.) Poly-caprolactone and its copolymers: Biodegradable polymers as drug delivery systems, Marcel Dekker, New York
16. Li G, Zhang H, Wang R, He Y, Xiong Y (2013) Preparation and antioxidant activity of albumin binding salen schiff-base metal complexes. Chinese Sci Bull 58:2956–2963
17. Wang R, He N, Song P, He Y, Ding L, Lei Z (2009) Preparation of nano-chitosan Schiff-base copper complexes and their anticancer activity. Polym Advan Technol 20:959–964
18. Komatsu T, Wang R, Zunszain PA, Curry S, Tsuchida E (2006) Photosensitized reduction of water to hydrogen using human serum albumin complexed with zinc-protoporphyrin IX. J Am Chem Soc 128:16297–16301
19. Wang RM, Song JF, He YF, Mao JJ, Li Y (2006) Conjugation of chitooligosaccharide-5-fluorouracil with bovine serum albumin. Chinese Chem Lett 17:1495–1498
20. Howe DH, Hart JL, McDaniel RM, Taheri ML, Magenau AJD (2018) Functionalization-induced self-assembly of block copolymers for nanoparticle synthesis. ACS Macro Lett 7:1503–1508
21. Cativo MHM, Kim DK, Riggleman RA, Yager KG, Nonnenmann SS, Chao H, Bonnell DA, Black CT, Kagan CR, Park S (2014) Air-liquid interfacial self-assembly of conjugated block copolymers into ordered nanowire arrays. ACS Nano 8:12755–12762
22. Pennakalathil J, Hong J (2011) Self-standing polyelectrolyte multilayer films based on light-triggered disassembly of a sacrificial layer. ACS Nano 5:9232–9237
23. Khapli S, Kim JR, Montclare JK, Levicky R, Porfiri M, Sofou S (2009) Frozen cyclohexane-in-water emulsion as a sacrificial

template for the synthesis of multilayered polyelectrolyte microcapsules. Langmuir 25:9728–9733
24. Tajbakhsh S, Hajiali F, Maric M (2020) Nitroxide-mediated miniemulsion polymerization of bio-based methacrylates. Ind Eng Chem Res 59:8921–8936
25. Nauman N, Zaquen N, Junkers T, Boyer C, Zetterlund PB (2019) Particle size control in miniemulsion polymerization via membrane emulsification. Macromolecules 52:4492–4499
26. Wang W, Zhang K, Chen D (2018) From tunable DNA/polymer self-assembly to tailorable and morphologically pure core-shell nanofibers. Langmuir 34:15350–15359
27. Jose LM, Kuriakose S (2019) Spectroscopic and thermal investigation of silver nanoparticle dispersed biopolymer matrix bovine serum albumin: A promising antimicrobial agent against the pathogenic bacterial strains. Macromol Res 27:670–678
28. Ghorbani M, Hamishehkar H, Tabibiazar M (2018) BSA/chitosan polyelectrolyte complex: A platform for enhancing the loading and cancer cell-uptake of resveratrol. Macromol Res 26:808–813
29. Kim D-Y, Shin W-S (2009) Roles of fucoidan, an anionic sulfated polysaccharide on bsa-stabilized oil-in-water emulsion. Macromol Res 17:128–132
30. Cho H, Lee T, Yoon J, Han Z, Rabie H, Lee KB, Su WW, Choi J (2018) Magnetic oleosome as a functional lipophilic drug carrier for cancer therapy. ACS Appl Mater Inter 10:9301–9309
31. Han L, Xia J, Hai X, Shu Y, Chen X, Wang J (2017) Protein-stabilized gadolinium oxide-gold nanoclusters hybrid for multimodal imaging and drug delivery. ACS Appl Mater Inter 9:6941–6949
32. Fu Y, Li Y, Li G, Yang L, Yuan Q, Tao L, Wang X (2017) Adaptive chitosan hollow microspheres as efficient drug carrier. Biomacromol 18:2195–2204
33. Rammohan A, Mishra G, Mahaling B, Tayal L, Mukhopadhyay A, Gambhir S, Sharma A, Sivakumar S (2016) PEGylated carbon nanocapsule: A universal reactor and carrier for in vivo delivery of hydrophobic and hydrophilic nanoparticles. ACS Appl Mater Inter 8:350–362
34. Chu D, Song X, Tan L, Ma H, Pang H, Wang X, Guo D (2019) Polyvinyl pyrrolidone-induced assembly of NiCo-LDHs nanosheets: A facile method for fabricating threedimensional flower-like microspheres with excellent supercapacitor performance. Inorg Chem Commun 110:107587–107614
35. Maciejewska M, Kolodynska D (2015) Synthesis and characterization of porous microspheres bearing pyrrolidone units. Mater Chem Phys 149–150:43–50
36. Wei H, Yang Z, Chen Y, Chu H, Zhu J, Li Z (2010) Characterisation of N-vinyl-2-pyrrolidone-based hydrogels prepared by a Diels-Alder click reaction in water. Eur Polym J 46:1032–1039
37. Chawathe M, Asheghali D, Minko S, Jonnalagadda S, Sidorenko A (2020) Adaptive hybrid molecular brushes composed of chitosan, polylactide, and poly(n-vinyl pyrrolidone) for support and guiding human dermal fibroblasts. ACS Appl Bio Mater 3:4118–4127
38. Nandy K, Srivastava A, Afgan S, Deepak KR, Rawat AK, Singh R, Singh RK (2020) The benzyl ethyl trithiocarbonate mediated control synthesis of a block copolymer containing N-vinyl pyrrolidone by RAFT methodology: Influence of polymer composition on cell cytotoxicity and cell viability. Eur Polym J 122:109387–109414
39. Godakanda VU, Li H, Alquezar L, Zhao L, Zhu L, de Silva R, Nalin de Silva KM, Williams GR (2019) Tunable drug release from blend poly(vinyl pyrrolidone)-ethyl cellulose nanofibers. Int J Pharmaceut 562:172–179
40. Sütekin SD, Güven O (2019) Application of radiation for the synthesis of poly(n-vinyl pyrrolidone)nanogels with controlled sizes from aqueous solutions. Appl Radiat Isotopes 145:161–169